

Simulation and application of site-selective optical spectroscopy to chromium-doped gadolinium garnets

This article has been downloaded from IOPscience. Please scroll down to see the full text article.

1990 J. Phys.: Condens. Matter 2 9639

(<http://iopscience.iop.org/0953-8984/2/48/017>)

View [the table of contents for this issue](#), or go to the [journal homepage](#) for more

Download details:

IP Address: 171.66.16.151

The article was downloaded on 11/05/2010 at 07:01

Please note that [terms and conditions apply](#).

Simulation and application of site-selective optical spectroscopy to chromium-doped gadolinium garnets

A Monteil

Laboratoire de Physico-Chimie des Matériaux Luminescents, Université Lyon I, Unité Associée au CNRS 442, Bâtiment 205, 43 Boulevard du 11 Novembre 1918, 69622 Villeurbanne Cédex, France

Received 11 October 1989, in final form 25 August 1990

Abstract. A simple mathematical model has been developed to simulate line narrowing spectroscopy. The application to different garnets doped with chromium is presented. A frequency shift effect due to non-resolved homogeneous and inhomogeneous lines of the same magnitude is observed and explained. The broadening of Cr^{3+} emission lines in gadolinium garnets is analysed in terms of interaction between paramagnetic ions.

1. Introduction

Since the first experiments of Szabo [1], site selection by means of fluorescence line narrowing (FLN) has become a useful method in spectroscopic experiments. It gives two main advantages by comparison with classical absorption or emission spectroscopy:

(i) It resolves inhomogeneous broadenings, which are always present in both crystalline and amorphous solids. It becomes possible to detect homogeneous lines and to determine their broadening mechanisms [2].

(ii) Site repartition and the influence of the crystal field can be studied [3].

Generally this technique is used when the homogeneous widths are much narrower than inhomogeneous ones ($\Delta\nu_h \ll \Delta\nu_{inh}$). This is the case, for instance, for crystal at low temperature or for glasses, which are largely inhomogeneous materials.

In this paper simulated and experimental results are presented in the case where the width of the residual narrowed line is of the order of the inhomogeneous broadening. Details of the application to gadolinium garnet crystals doped with chromium is given.

2. Mathematical model

In FLN experiments, the shape of emission lines is given by the convolution of absorption homogeneous lines and emission homogeneous lines [3]. A more complete treatment of such spectra is proposed, which can be used for any case occurring: emission, absorption, excitation spectrum, with or without site selection. In the following the influence of the apparatus (apparatus function or width) will be neglected. This can be done without affecting the generality of the results.

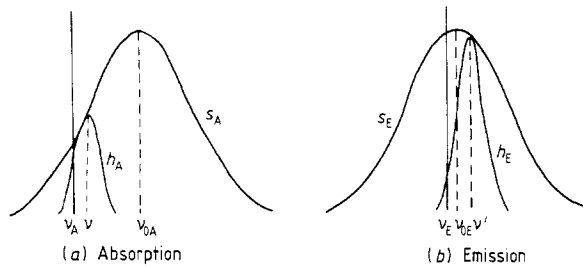


Figure 1. Schematic diagram of lineshape function used in this paper: (a) absorption, (b) emission.

Let us specify the notation: ν_A and ν_E for the absorption and emission frequencies; ν and ν' for the central frequencies of ions of classes C for absorption and C' for emission. 'Class' refers to a set of ions belonging to the same site, under the influence of the same crystalline environment.

The homogeneous shape functions are h_A and h_E . The inhomogeneous repartition functions of ion classes, are s_A and s_E with central frequencies ν_{0A} and ν_{0E} respectively.

The intensity of absorption $A(\nu, \nu_A)$ for all ions of a class C at a frequency ν_A (figure 1(a)) is equal to the probability for such a class to absorb at that frequency [$h_A(\nu_A - \nu)$] times the number of ions of that class [$s_A(\nu - \nu_{0A})$]; we find

$$A(\nu, \nu_A) = h_A(\nu_A - \nu)s_A(\nu - \nu_{0A}). \quad (1)$$

The intensity $A(\nu, \nu_A)$ cannot be experimentally measured since at a given frequency several classes can absorb. So, the absorption line shape is found by integration over all classes:

$$I_A(\nu_A) = \int A(\nu, \nu_A) d\nu = \int h_A(\nu_A - \nu)s_A(\nu - \nu_{0A}) d\nu. \quad (2)$$

The inhomogeneous line is the convolution product of the homogeneous line with the sites repartition function.

In the same way, determining the intensity of emission $E(\nu', \nu_E)$ for all of ions of a given class C' at the frequency ν_E without taking the excitation channel into account or with the assumption that all classes have been excited in the same way (figure 1(b)), we get the product of the probability of that class to emit at that frequency [$h_E(\nu_E - \nu')$] by the number of ions of the class in the system [$s_E(\nu' - \nu_{0E})$]:

$$E(\nu', \nu_E) = h_E(\nu_E - \nu')s_E(\nu' - \nu_{0E}). \quad (3)$$

Such an intensity cannot be measured and an integration over all classes is needed. The inhomogeneous line for emission comes from the convolution between the homogeneous line and the site repartition function

$$I_E(\nu_E) = \int E(\nu', \nu_E) d\nu' = \int h_E(\nu_E - \nu')s_E(\nu' - \nu_{0E}) d\nu'. \quad (4)$$

Now we combine the absorption at ν_A of a class C with the emission at ν_E of a class C', and we get the intensity of emission taking account of absorption. The intensity of emission $F(\nu_E, \nu', \nu_A, \nu)$ for all ions in a given class C' at a frequency ν_E that follows

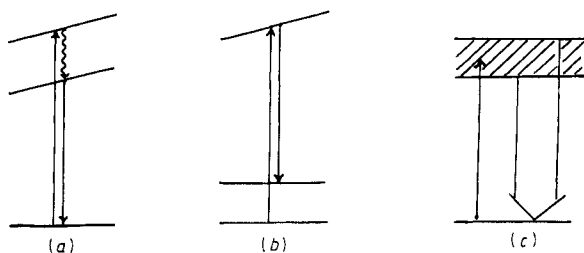


Figure 2. Schematic diagram of energy levels illustrating different FLN cases discussed in the text. (a) Absorption–relaxation–emission. (b) Absorption and emission on different levels. In both cases the slope of the excited energy levels indicates the inhomogeneous broadening of these levels. (c) Absorption and emission when the homogeneous broadening of the excited state is predominant.

the absorption in a class C at a frequency ν_A is proportional to both processes $A(\nu, \nu_A)$ and $E(\nu', \nu_E)$:

$$F(\nu_E, \nu', \nu_A, \nu) = h_A(\nu_A - \nu) s_A(\nu - \nu_{0A}) h_E(\nu_E - \nu') s_E(\nu' - \nu_{0E}). \quad (5)$$

This last equation looks as if there is no relation between the two processes; it is obviously not true. It is clear that there should be some relationship between classes C and C'. The kind of correspondence between them could be as follows: classes C and C' are the same, but the frequencies ν and ν' are not resonant. This is the case when we have a process such as absorption–relaxation–emission (figure 2(a)) or when emission occurs on a split level (figure 2(b)). It occurs more simply when the frequencies ν and ν' are also identical; this is the case for resonant excitation. Another case which might occur could be a correlation between processes themselves. In this treatment the cases where emission and absorption are not independent (as in second-order phenomena) have been ignored.

In order to determine the shapes of lines we integrate expression (5) over all the classes, but because of the different relationships between the classes C and C' the integration cannot be done in the same way. Let us write

$$I(\nu_E, \nu_A) = \iint F(\nu_E, \nu', \nu_A, \nu) d\nu d\nu'. \quad (6)$$

This final expression gives all the known results concerning absorption and emission line shapes (particularly in FLN experiments), and, moreover, it can predict new results.

2.1. Broad band absorption

With a broad band absorption, ions belonging to all classes C are excited in the same way. In relation (6) absorption and emission can be separated and by integration over the frequency ν_A we get

$$\begin{aligned} I_E(\nu_E) &= \int I(\nu_E, \nu_A) d\nu_A = \iint A(\nu, \nu_A) d\nu_A d\nu E(\nu', \nu_E) d\nu' \\ &= \text{constant} \int E(\nu', \nu_E) d\nu'. \end{aligned}$$

We obtain relation (4) again for the inhomogeneous line for emission. The evident result is that it is not possible to perform site selection with broad band excitation.

2.2. FLN with $\Delta\nu_{hA} \gg \Delta\nu_{inhA}$

When the homogeneous broadening in absorption is large compared to the inhomogeneous effects, the repartition function s_A can be considered as a Dirac function for the homogeneous function h_A . This case occurs, for instance, when the excitation is performed in a large absorption band (figure 2(c)) such as the ${}^4A_2 \rightarrow {}^4T_2$ transition of Cr^{3+} . The elimination of ν in (6) gives

$$I_E(\nu_E) = h_A(\nu_A - \nu_{0A}) \int E(\nu', \nu_E) d\nu'$$

where we can see that the shape of emission is that of the inhomogeneous line in expression (4). Here it is still impossible to perform site selection. Such a case has been shown experimentally for ruby [4].

2.3. FLN with $\Delta\nu_{hE} \gg \Delta\nu_{inhE}$

When the homogeneous broadening in emission is large compared to the inhomogeneous effects, we get a result comparable with the previous one: the shape of emission is that of the homogeneous line for emission

$$I_E(\nu_E) = h_E(\nu_E - \nu_{0E}) \int A(\nu, \nu_A) d\nu$$

or

$$I_E(\nu_E) = \text{constant} \times h_E(\nu_E - \nu_{0E}).$$

Here, too, the mathematical model allows us to find some well known experimental properties to be reproduced.

2.4. FLN with identity and resonance between classes C and C'

This is the most common case for FLN experiments and corresponds to an extension of the results given by Riseberg [3] to the case where inhomogeneous broadening is not dominant. Supposing that ν and ν' are identical, firstly we write

$$I(\nu_E, \nu_A) = \int h_A(\nu_A - \nu) s_A(\nu - \nu_{0E}) h_E(\nu_E - \nu) s_E(\nu - \nu_{0E}) d\nu. \quad (7)$$

Secondly, considering that the h and s functions are identical for absorption and emission, we write

$$I(\nu_E, \nu_A) = \int h(\nu_A - \nu) s^2(\nu - \nu_0) h(\nu_E - \nu) d\nu. \quad (7a)$$

This expression is different from that developed by Riseberg [3]. Note the presence

of s^2 . If s varies more slowly than h , that is to say the inhomogeneous broadening is predominant, we find again the expression given by Riseberg.

2.5. FLN without resonance but with identical classes C and C'

This is an interesting and also useful case where absorption and emission are related, for instance, through a relaxation mechanism which, however, keeps the identity of classes C and C'. Let us call $\Delta\nu$ the gap $\nu - \nu'$. In general $\Delta\nu$ is positive at low temperatures (Stokes emission). We obtain

$$I(\nu_E, \nu_A) = \int h_A(\nu_A - \nu) s_A(\nu - \nu_{0A}) h_E(\nu_E - \nu + \Delta\nu) s_E(\nu - \Delta\nu - \nu_{0E}) d\nu \quad (8)$$

or, eliminating ν , an equivalent expression with only ν' .

It is worth noting that relations (6)–(8) are functions dependent on ν_A and ν_E , thus they can be considered as a function of ν_E for emission: $I_{\nu_A}(\nu_E)$, or as a function of ν_A for excitation spectroscopy: $I_{\nu_E}(\nu_A)$.

In the more simple case of identity and resonance between classes and considering the case where the inhomogeneous broadening is dominant, expression (7) will give the same result as the expression developed by Riseberg [3]. That is to say, the line shape of the FLN emission is given simply by the convolution of the homogeneous line-shape functions for the absorption and the emission:

$$I(\nu_E, \nu_A) = \text{constant} \times \int h_A(\nu_A - \nu) h_E(\nu_E - \nu) d\nu.$$

It appears that if the inhomogeneous broadening is not dominant, the previous sentence and the related expression are no longer valid.

3. Applications

In this section some applications of the earlier results are presented. The purpose is both to explain some well known experimental results and to predict some new ones.

3.1. FLN in the case of ruby ($Al_2O_3:Cr^{3+}$)

The emission of ruby at low temperature is mainly due to the transition between ${}^2E(\bar{E})$ and ${}^4A_2(\pm\frac{3}{2}, \pm\frac{1}{2})$ states which gives two lines (figure 3). In general the splitting of the ground state ($\delta = 0.38 \text{ cm}^{-1}$) is hidden by the inhomogeneous broadening. Let us call the two transitions α and β , and the four possible processes 1, 2, 3 and 4:

1	Absorption α	Emission α
2	Absorption α	Emission β
3	Absorption β	Emission α
4	Absorption β	Emission β

We get for the emission intensity

$$I_1 = \int h_A(\nu_A - \nu) s_A(\nu - \nu_{0\alpha}) h_E(\nu_E - \nu) s_E(\nu - \nu_{0\alpha}) d\nu$$

$$I_2 = \int h_A(\nu_A - \nu) s_A(\nu - \nu_{0\alpha}) h_E(\nu_E - \nu + \delta) s_E(\nu - \delta - \nu_{0\beta}) d\nu$$

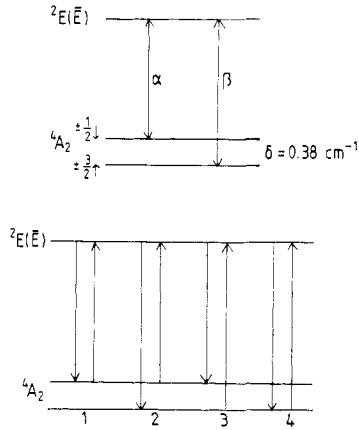


Figure 3. Schematic diagram of energy levels showing the two transitions and four processes discussed in the text for ruby (α $\text{Al}_2\text{O}_3:\text{Cr}^{3+}$).

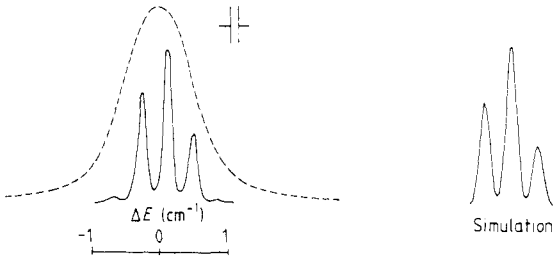


Figure 4. Line-narrowing emission spectra of the ${}^2\text{E}(\bar{\text{E}}) \rightarrow {}^4\text{A}_2$ transition of ruby at helium temperature. The broken curve represents the inhomogeneous emission. The simulated spectrum was calculated using the expressions developed in the text. Gaussian functions were simply taken for h and s functions.

$$I_3 = \int h_A(\nu_A - \nu + \delta) s_A(\nu - \delta - \nu_{0\beta}) h_E(\nu_E - \nu) s_E(\nu - \nu_{0\alpha}) d\nu$$

$$I_4 = \int h_A(\nu_A - \nu + \delta) s_A(\nu - \delta - \nu_{0\beta}) h_E(\nu_E - \nu + \delta) s_E(\nu - \delta - \nu_{0\beta}) d\nu$$

where $\nu_{0\alpha}$ and $\nu_{0\beta}$ are the central frequencies for the transition α and β , of which we know that the gap is δ . If, by simplification, we consider the functions h as Dirac functions with regard to the inhomogeneous s functions, we get the results

$$\begin{aligned} I_1 &= s_A(\nu_A - \nu_{0\alpha}) s_E(\nu_E - \nu_{0\alpha}) && \text{with } \nu_A = \nu_E \\ I_2 &= s_A(\nu_A - \nu_{0\alpha}) s_E(\nu_E - \nu_{0\beta}) && \text{with } \nu_A = \nu_E + \delta \\ I_3 &= s_A(\nu_A - \nu_{0\beta}) s_E(\nu_E - \nu_{0\alpha}) && \text{with } \nu_A = \nu_E - \delta \\ I_4 &= s_A(\nu_A - \nu_{0\beta}) s_E(\nu_E - \nu_{0\beta}) && \text{with } \nu_A = \nu_E. \end{aligned}$$

Giving an expression to the s functions and a value to $\nu_{0\alpha}$, $\nu_{0\beta}$, ν_A or ν_E it is easy to compute the intensities I_1 to I_4 . It follows that for a given frequency of absorption, the emission occurs at three different frequencies. This result is well known from the experiments of Selzer *et al* [5]. Figure 4 shows an experimental spectrum of FLN together with a simulated one. The simulation was done using the precedent relations and Gaussian function for the h functions. In this case the homogeneous width is not reached and the h functions represent the apparatus resolution. The s functions are chosen in order to fit the inhomogeneous line shape of the sample. The sample of ruby $\text{Al}_2\text{O}_3:\text{Cr}^{3+}$

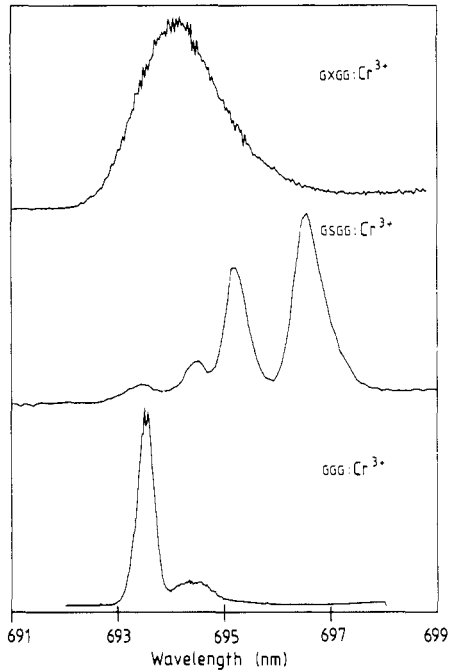


Figure 5. Experimental inhomogeneous emission from the ${}^2E \rightarrow {}^4A_2$ Cr^{3+} transition of three different garnets: $Gd_3(Ca, Mg, Zr)_2Ga_3O_{12}$ (GXGG), $Gd_3Sc_2Ga_3O_{12}$ (GSGG) and $Gd_3Ga_5O_{12}$ (GGG) at 6 K.

(0.1 wt%) has been used because of the wide breadth of its linewidth due to a basal plastic deformation (J L Cadoz, Laboratoire de Physique des Matériaux, Meudon, France).

3.2. FLN in the case of a chromium-doped gadolinium garnet

In earlier papers some results are given on FLN in garnets like $Gd_3(Ca, Mg, Zr)_2Ga_3O_{12}$ [6], which will be called GXGG in the text below, or $Gd_3Sc_2Ga_3O_{12}$ (GSGG) [7] or $Gd_3Ga_5O_{12}$ (GGG) [7] all of them doped by chromium. A peculiarity of these crystals is an important broadening of the transition ${}^2E \rightarrow {}^4A_2$ at low temperature which is due in part to the inhomogeneity as it was discussed by Struve and Huber [8] in GSGG and GGG. This effect is particularly important in GXGG where several different cations of different ionic radii increase the lattice distortions and by consequence the inhomogeneity. Figure 5 shows the 2E emission spectra of different garnets at low temperature.

However, another peculiarity of these garnets is to have a 2E FLN emission with a rather broad 'homogeneous' width (specifically we have measured widths of 7–12 cm^{-1}). This peculiarity is due to the gadolinium always present in the lattice and will be discussed in the next part of the paper.

Let us apply the relation (8) derived above. In this case the splitting of the ground state 4A_2 cannot be seen. The 2E state is split in two levels by the effect of a trigonal field and spin-orbit interaction. The splitting Δ is commonly of the order of 30 to 40 cm^{-1} . Let us label the two possible transitions α and β instead of the usual R_1 and R_2 . Due to the value of the splitting Δ only two processes are possible (figure 6):

- | | | |
|---|---------------------|--------------------|
| 1 | Absorption α | Emission β |
| 2 | Absorption β | Emission β . |

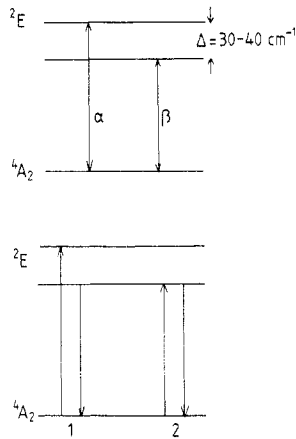


Figure 6. Schematic diagram of energy levels showing the two transitions and the two processes discussed in the text for garnets.

The two different intensities are

$$I_1 = \int h_A(\nu_A - \nu) s_A(\nu - \nu_{0\alpha}) h_E(\nu_E - \nu + \Delta) s_E(\nu - \Delta - \nu_{0\beta}) d\nu \quad (9)$$

$$I_2 = \int h_A(\nu_A - \nu + \Delta) s_A(\nu - \Delta - \nu_{0\beta}) h_E(\nu_E - \nu + \Delta) s_E(\nu - \Delta - \nu_{0\beta}) d\nu. \quad (10)$$

By the same simplification as in the ruby case we obtain

$$I_1 = s_A(\nu_A - \nu_{0\alpha}) s_E(\nu_E - \nu_{0\beta}) \quad \text{with } \nu_A = \nu_E + \delta \quad (11)$$

$$I_2 = s_A(\nu_A - \nu_{0\beta}) s_E(\nu_E - \nu_{0\beta}) \quad \text{with } \nu_A = \nu_E. \quad (12)$$

For a given absorption frequency the emission is composed of two lines even at low temperature but only when the inhomogeneous width is larger than the splitting Δ . On figure 7 is drawn the FLN spectrum for GXGG as an illustration of this discussion. The simulated spectrum is also plotted on the same figure. In this case homogeneous width is taken in order to fit the experimental curve.

For a given emission frequency the excitation (absorption) is performed at two different frequencies. This result is well known and is used widely to measure the splitting of the 2E state. Figure 8 shows an example of such a GGG excitation spectrum with its simulation.

When the residual width in FLN experiments is of the same order as the inhomogeneous one, it is preferable to use expressions (9) and (10) (rather than (11) and (12)) for simulation calculations. Several simulations have been performed using the right expressions, in the case where the 'homogeneous' width is of the same magnitude as the inhomogeneous one. On the one hand, the simulations of emission spectra were done choosing an 'absorption frequency' ν_A in the way it is done by laser excitation and computing the emission spectrum with the relations developed before. By 'tuning' the absorption frequency, that is to say by using different values for that frequency, we obtained different spectra. On the other hand, simulated excitation spectra were given with the 'emission frequency' ν_E as the chosen parameter, in the way as we set the

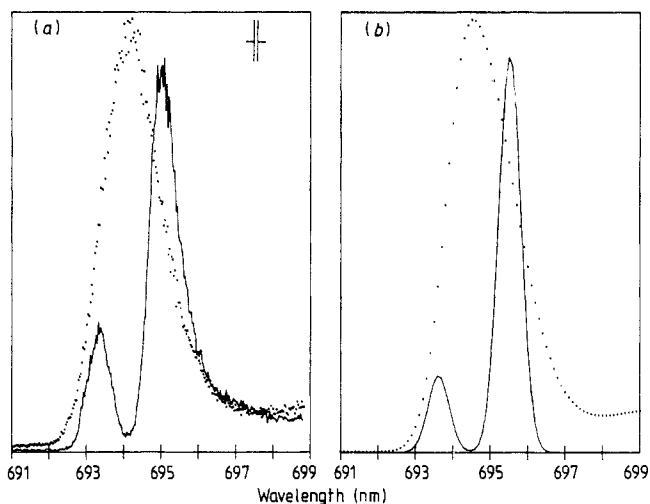


Figure 7. Line narrowing emission spectra of the ${}^2E \rightarrow {}^4A_2$ transition of $GxGG:Cr^{3+}$ at helium temperature. (a) Experimental spectra, (b) simulated spectra. The dotted curve represents the inhomogeneous emission. The simulated spectrum was computed using the expressions developed in the text. A Gaussian function was used for h functions and a function for s adequate to fit the inhomogeneous emission.

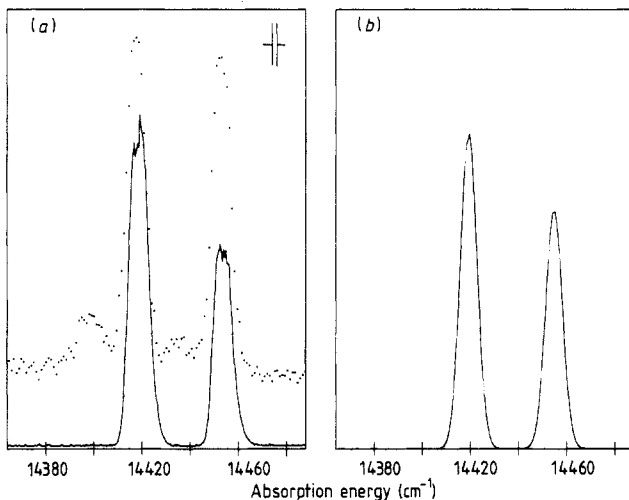


Figure 8. Line narrowing excitation spectra of the ${}^2E \leftarrow {}^4A_2$ transition of $GGG:Cr^{3+}$ at 6 K. The dotted curve represents the inhomogeneous absorption. (a) Experimental spectra, (b) simulated spectra. The simulated spectrum was calculated using the expressions developed in the text. Gaussian functions were used for h and s functions.

monochromator at a fixed position when recording an excitation spectrum. The result for $GGG:Cr^{3+}$ is presented in figure 9. Let us note that the inhomogeneous emission of GGG (figure 5) is composed by one main line and a satellite. This second line is due to

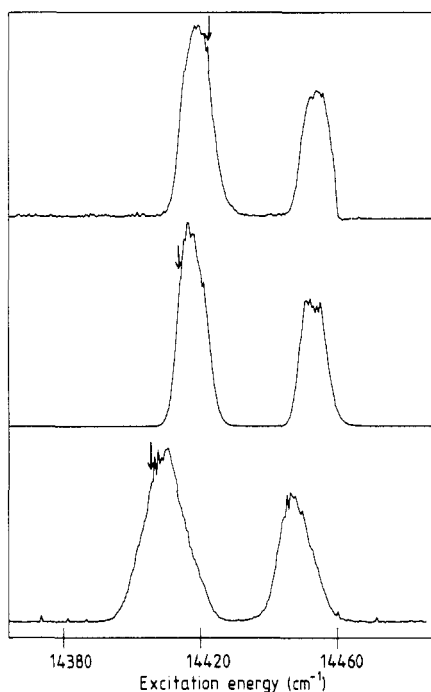


Figure 9. Line narrowing excitation spectra of the ${}^2E \leftarrow {}^4A_2$ transition of $\text{GGG}:\text{Cr}^{3+}$ at 6 K. Each spectrum corresponds to a different emission wavelength. Emission positions are indicated by arrows. Notice the shift of the maximum.

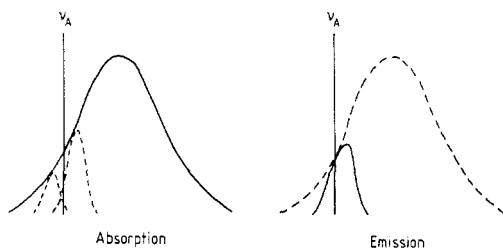


Figure 10. Schematic diagram of lineshape in the case of a broad homogeneous width. The broken curves in the absorption diagram represent h functions for different absorbing sites. In the emission diagram they give a shifted line (full curve).

different sites for chromium [8]. The simulation that is presented takes account of these sites, but not of the energy transfer between them.

An important observation is that the maximum of emission is no longer resonant with the excitation but is shifted towards the centre of the inhomogeneous line. Such an effect can be explained in figure 10: when the excitation stands on a wing of an inhomogeneous line, due to a broad homogeneous width, several classes of ions are excited. However, classes with the maximum nearer to the centre are more numerous and consequently their emission is stronger and the emission envelope is shifted towards the centre.

This shift can be seen clearly on some of the spectra where the diffusion of the exciting laser appears (figure 11). The variation of the shift with the position of the emission frequency (in the case of excitation spectra) is presented and compared with the results on GGG. One can see in figure 12 the agreement between experiment and simulation. The discrepancy between measurements and simulations for the low energy satellite peak comes from the more complicated structure of this peak due to several sites [7].

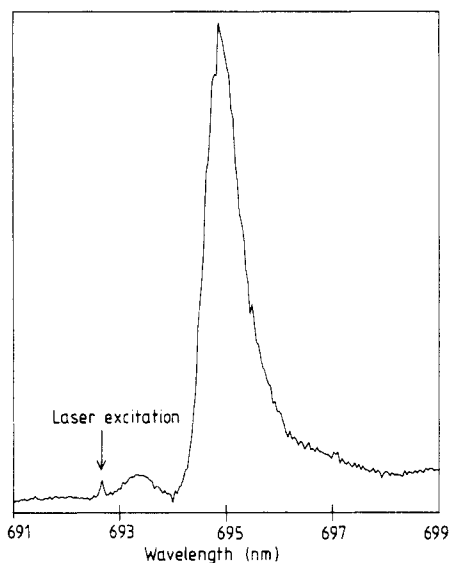


Figure 11. Line narrowing spectrum for GGG showing the laser excitation position (arrowed) and the emission shift.

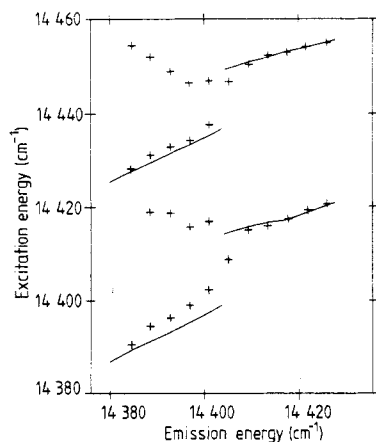


Figure 12. Plot of the experimental position of the maxima in excitation spectra for GGG. The full curves represent the calculated values. Crosses without curves correspond to supplementary peaks due to energy transfer.

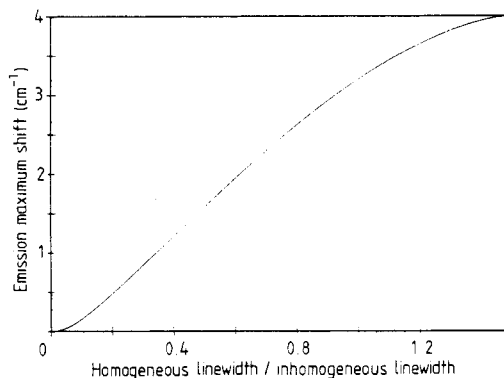


Figure 13. Variation of the shift between absorption and the emission maximum with the ratio between homogeneous and inhomogeneous linewidths. The s and h functions are taken as Gaussian functions (Lorentzian functions could be used for h functions). $\Delta\nu_{\text{inh}} = 10 \text{ cm}^{-1}$ and $\nu_A - \nu_{0A} = 5 \text{ cm}^{-1}$.

It is evident that this effect depends strongly on the ratio between homogeneous and inhomogeneous width. The result of several simulations with different ratios is plotted on figure 13. This emphasizes the fact that in the convolution between absorption and emission we need both the homogeneous and the inhomogeneous line shape.

4. Origin of homogeneous broadening

It has been stated in previous papers [6–7] and in section 3 of this paper that for GGG-like chromium-doped garnets we were unable to perform FLN experiments with lines

narrower than a few cm^{-1} . This origin of the homogeneous broadening is well known [9], the main causes are phonon processes which are strongly temperature-dependent.

The transition of interest, ${}^2\text{E} \rightarrow {}^4\text{A}_2$ is forbidden, and its lifetime of some milliseconds is inconsistent with a homogeneous width of several cm^{-1} . Another cause of broadening is the spin–spin interaction [10] which gives the homogeneous width for ruby [11]. The usual values are too low to explain our ‘broad’ lines.

One common characteristic of these garnets is that gadolinium is a compound of the lattice, and Gd^{3+} is a paramagnetic ion. The spin–spin interaction by the surrounding nearest neighbours (Gd^{3+}) on the paramagnetic element (Cr^{3+}) will create a magnetic field of random direction and intensity in the lattice, this will split and shift randomly the levels of Cr^{3+} . This coupling between paramagnetic ions is known, for instance in the case of concentrated ruby, and it gives several lines of Cr^{3+} pairs shifted from the R lines of single ions.

The mean magnetic field between two paramagnetic ions, ≈ 0.3 nm apart, is of the order of $(\mu_0/4\pi)\beta r^{-3}$, which may be 10^{-2} T or so [10] (β is the Bohr magneton). In the case of Gd^{3+} , for which the magnetic moment is 7β , the local field will be higher. However, it is conceivable that the effects of the Gd^{3+} nearest neighbours of a Cr^{3+} ion partially cancel one another (if there is no magnetic order), so the magnetic field seen by a Cr^{3+} ion would be lower than the sum of the neighbours’ contribution, in the order of 1 T. The most likely splitting that can be predicted with such a field value is about 1 cm^{-1} , that is not too far from the observed values; the local field seems to be a little stronger. In the macroscopic range random variations of the microscopic magnetic field and then of the splitting for each ion broadens the lines without correlation with the inhomogeneous broadening due mainly to local variations of the electrostatic crystal field. Even if the internal magnetic field contributes to the inhomogeneous broadening, there is no correlation between it and the crystal field. An absorption in a given energy corresponds to the absorption of different classes of ions that would be at different energies in the absence of a magnetic field, but whose levels are shifted and split by the magnetic field to create a level at that energy. The associated emission will be at different wavelengths coming from these different split levels. In consequence site selection by line narrowing spectroscopy does not permit a narrowing of lines beyond the mean Zeeman splitting due to the mean magnetic field. The width of the narrowed line gives a magnitude for the mean magnetic field.

If this effect is really due to the interaction of gadolinium and chromium ions via a magnetic field it should be seen in other compounds of gadolinium doped with chromium. However, such a compound must not have too weak a crystal field if FLN measurements are to be made on the ${}^2\text{E}$ state. The ${}^4\text{T}_2$ state is very sensitive to the crystal field and when the crystal field is weak this state is lower than the ${}^2\text{E}$ state. In this case only the emission from the ${}^4\text{T}_2$ is seen as a very broad band which cannot be narrowed due to the large homogeneous width of the band.

From the same point of view, garnets having the same structure but without gadolinium must not present such broad ‘narrowed’ lines. This is effectively the case for $\text{Y}_3\text{Al}_5\text{O}_{12}$ (YAG) doped with chromium for which we have found narrowed line widths limited by the apparatus resolution [12].

5. Conclusion

A mathematical model for line narrowing spectroscopy has been developed. It allows easy simulation of experimental emission or excitation spectra. The main conclusion to

be drawn is that when homogeneous and inhomogeneous broadenings are of the same magnitude, emission and excitation are no longer resonant, even in resonant experiments. Such an effect must be carefully distinguished from processes such as spectral energy transfer. Several examples taken from the spectra of Cr^{3+} doped garnets have been explained in this paper or have been given as illustration of such an effect.

The apparent broad homogeneous line for gadolinium garnets has been explained as an effect of the paramagnetic gadolinium splitting in several Zeeman sub-levels in chromium ions. The width of the narrowed lines gives a measurement of the mean magnetic field. To go beyond these broad lines it would be useful to apply an external magnetic field. By lining up all magnetic spins non-random values will be obtained for Zeeman splitting and narrower lines will be obtained as demonstrated by Jessop *et al* in ruby [11].

Note added in proof:

Recent experiments have been done on $\text{Cr}^{3+} : \text{GGG}$ under a magnetic field. The initial results show that we obtain a narrower line than without a magnetic field, as was predicted above [13].

Acknowledgment

The author is grateful to E Duval for numerous illuminating discussions.

References

- [1] Szabo A 1970 *Phys. Rev. Lett.* **25** 924
- [2] Dubost H, Charneau R and Harig M 1982 *Chem. Phys.* **69** 389
- [3] Riseberg L A 1973 *Phys. Rev. A* **7** 671
- [4] Monteil A and Duval E 1979 *J. Lumin.* **18/19** 793
- [5] Selzer P M, Huber D L, Barnett B B and Yen W M 1978 *Phys. Rev. B* **17** 4979
- [6] Monteil A, Garapon C and Boulon G 1988 *J. Lumin.* **39** 167
- [7] Monteil A, Nie W, Madej C and Boulon G 1990 *Opt. Quantum Electron.* **22** S247
- [8] Struve B and Huber G 1985 *Appl. Phys. B* **36** 195
- [9] McCumber D E and Sturge M D 1963 *J. Appl. Phys.* **34** 1682
- [10] Abragam A and Bleaney B 1970 *Electron Paramagnetic Resonance of Transition Ions* (Oxford: Clarendon) p 491
- [11] Jessop P E, Muramoto T and Szabo A 1980 *Phys. Rev. B* **21** 966
- [12] Nie W, Boulon G and Mareš J 1989 *Chem. Phys. Lett.* **160** 597
- [13] Ferrari M, Rossi F and Monteil A unpublished